The authors wish to thank Professor J. Chikawa and the Photon Factory for providing the opportunity to carry out this work. The authors are most grateful to Professors H. Iwasaki and T. Matsushita of the Photon Factory for their encouragement, Dr A. Pogany for arranging the ion implantation of the Si sample, Dr S. Prawer for the Monte Carlo calculation and Dr S. Sasaki for supplying the Si analyzer crystal used at the Photon Factory. Two of the authors (AWS, SWW) gratefully acknowledge financial support from the Australian Department of Science under the Japan/Australia Bilateral Exchange Program.

References

Afanas'ev, A. M., Aleksandrov, P. A., Fanchenko, S. S., Chaplanov, V. A. & Yakimov, S. S. (1986). *Acta Cryst.* A42, 116-122.

Afanas'ev, A. M., Koval'chuk, M. V., Kovev, E. K. & Kohn, V. G. (1977). *Phys. Status Solidi A*, **42**, 415-422.

Andrews, S. R. & Cowley, R. A. (1985). *J. Phys. C*, **18**, 6427-6439.

Cowley, R. A. & Ryan, T. W. (1987). *J. Phys D*, **20**, 61-68.

Eisenberger, P., Alexandropoulos, N. G. & Platzman, P. M. (1972). *Phys. Rev. Lett.* **28**, 1519-1522.

Iida, A. & Kohra, K. (1979). *Phys. Status Solidi A*, **51**, 533-541.

Kashiwagura, N., Kashihara, Y., Sakata, M., Harada, J., Wilkins, S. W. & Stevenson, A. W. (1987). *Jpn. J. Appl. Phys.* **26**, L2026-L2029.

Kim, H., Gotoh, S. J., Takahashi, T., Ishikawa, T. & Kikuta, S. (1986). *Nucl. Instrum. Methods*, **A246**, 810-813.

Matsushita, T., Ishikawa, T. & Oyanagi, H. (1986). *Nucl. Instrum. Methods*, **A246**, 377-379.

Robinson, I. K. (1986). *Phys. Rev. B*, **33**, 3830-3836.

Wilkins, S. W., Chadderton, L. T. & Smith, T. F. (1983). *Acta Cryst.* **A39**, 792-800.

Yakimov, S. S., Chaplanov, V. A., Afanas'ev, A. M., Aleksandrov, P. A., Imamov, R. M. & Lomov, L. A. (1984). *JETP Lett.* **39**, 1-3.

Zaumseil, P. (1985). *Phys. Status Solidi A*, **91**, K31-K33.

Acta Cryst. (1988). A**44**, 833-837

Reflection and Refraction of Fast Electrons at Solid/Solid Interfaces

By J. Taftø

Research Centre, Norsk Hydro a.s, 3901 Porsgrunn, Norway

and J. Gjønnes

Department of Physics, University of Oslo, Blindern, Oslo, Norway

(*Received* 15 *December* 1987; *accepted* 18 *April* 1988)

Abstract

The combined effects of refraction and reflection of fast electrons entering a thin specimen nearly parallel to an interface may be used to obtain quantitative information about the difference in the mean inner Coulomb potential (U_0) between the two adjoining phases. When no strong Bragg reflections are excited the electrons are deflected towards the phase with the largest $|U_0|$. By tilting the crystal so that strong Bragg reflections are excited some of the Bloch waves may be deflected in the opposite direction. The effect is demonstrated by simple two-beam calculations and observations for the Al/SiC interface.

Introduction

Whereas a variety of experimental techniques are available for the study of solid/vacuum interfaces, only a few methods are capable of providing information about buried interfaces. The most powerful technique for studying the structure of solid/solid interfaces may be TEM (transmission electron microscopy and diffraction). High-resolution imaging interpreted on the basis of the multi-slice formulation of Cowley & Moodie (1957) allows study of interface structures on an atomic scale (Ourmazd, Taylor, Rentschler & Bevk, 1987; Krakow, Wetzel & Smith, 1986). Several analytical techniques combined with a fine electron probe can be used to obtain profiles of composition on a nanometre scale. With electron energy-loss spectroscopy in particular, signals may be obtained from areas as small as 10 Å, including information about electronic structure as well (Batson, Kavangh, Wodall & Mayer, 1986).

In this paper we deal with a different TEM technique for extracting information about interfaces. The principle has been outlined briefly in a previous paper (Taftø, Jones & Heald, 1986). The deflection of the electron beam by the interface between two solids A and B due to the difference $\Delta U_0 = U_{0,A} - U_{0,B}$ between their mean inner potentials is used to form an image of the interface. This combined refraction/reflection effect may also be used to obtain electron energy loss spectra from the interfacial region.

The aim of the present paper is to present a further discussion of this technique, in particular the effect of Bragg reflection in one or both of the crystals and

0108-7673/88/060833-05$03.00

how this can be utilized for measurement of the inner potential U_0 and thus provide information about electronic structure.

Kinematical case: no Bragg reflection

There is no fundamental difference between these refraction and reflection effects and the refraction of electrons at an external surface. Specimen preparation may be more difficult when dealing with buried interfaces. On the other hand, there will be no need for the ultra-high vacuum which is often considered essential in the study of surface structures by TEM.

In the absence of Bragg reflections on either side, the internal (buried) interface can be described as a step in the refractive index due to the difference ΔU_0 between the inner potentials. For an incident beam nearly parallel to the interface, *i.e.* at a glancing angle less than the total reflection angle $\alpha = (\Delta U_0)^{1/2}/K$, the electrons will be either refracted or reflected by the interface, depending on the side on which they enter the specimen. K is here the wave vector of the incident electron with Å^{-2} as unit for the scattering potential U. The total reflection case, which means total internal reflection for an external surface, has been studied by Cowley & Turner (1981) at the surface of an MgO crystal cube.

The principle of the reflection/refraction at an interface is illustrated in Fig. 1. A nearly parallel beam enters the thin specimen in a region including an interface between the phases A and B. Within the total reflection range the beam will be refracted into and reflected within the phase A with the lower potential energy of the electron (*i.e.* higher electrostatic potential). Referring to Fig. 1(*b*), we see that the wave in A with wave vector component $K_{z,A}$ cannot penetrate into B and is totally reflected, whereas the wave in B will be refracted into A. In the diffraction pattern this will be seen as a faint streak on the side of the direct spot which is pointing towards phase A, *i.e.* towards the lower-potential side. This is shown in Fig. 1(*c*) for the interface Si(111)/SiO_2 (amorphous). This diffraction pattern is from a thin area, ~500 Å of an ion-thinned specimen with the incident beam parallel to the interface. The streak points towards the silicon side, showing that $|U_{0,\mathrm{Si}}| > |U_{0,\mathrm{SiO}_2}|$.

In-focus images with the objective aperture around the deflected streak near the direct beam can be used to mark the interface. This imaging technique is used to reveal a series of interfaces as shown in Fig. 2 for an ion-thinned cross section of an Si(100) wafer with 10–15 Å of native SiO_2, 40 Å of evaporated Cr and 1000 Å of evaporated Cu. In Fig. 2(*a*) the objective aperture was displaced towards the Si substrate and the Si/SiO_2 interface brightens up. Fig. 2(*b*) was taken with the objective aperture displaced in the opposite direction and the SiO_2/Cr and Cr/Cu interfaces brighten up. From these pictures it can be inferred that $|U_{0,\mathrm{Si}}| > |U_{0,\mathrm{SiO}_2}|$, $|U_{0,\mathrm{SiO}_2}| < |U_{0,\mathrm{Cr}}|$ and $|U_{0,\mathrm{Cr}}| < |U_{0,\mathrm{Cu}}|$.

Fig. 3 is taken from the SiC/Al interface in a commercial metal matrix composite. With the objective aperture displaced towards SiC (Fig. 3*a*) we observe an image similar to those in Fig. 2. By imaging with the electrons continuing in the forward direction, we observe the complementary image, Fig. 3(*b*).

Bragg reflection and dynamical scattering

When Bragg reflections are excited at either side of the interface the condition for refraction and reflection is changed. We can describe the resulting effects in terms of Bloch waves. The different Bloch waves

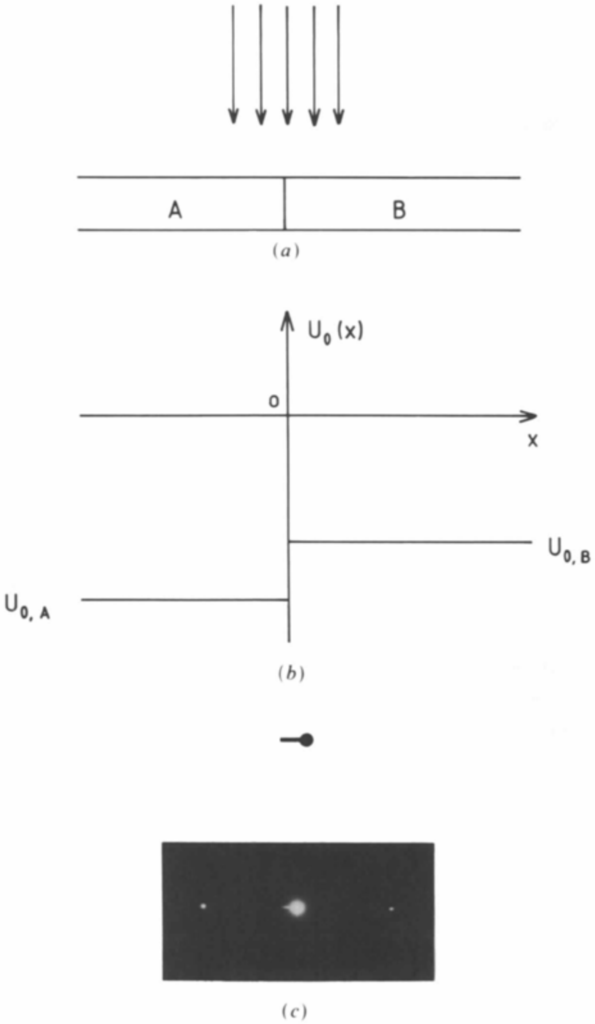

Fig. 1. (*a*) Interface region between two phases A and B. (*b*) The potentials of the fast electrons in A and B. (*c*) Schematic illustration of the deflection (streak) from the forward direction (filled circle), and observed deflection in the diffraction pattern from the Si(111)/SiO_2 interface when 120 keV electrons are incident parallel to the interface.

will be located in different parts of the crystal unit cell and hence see a different potential or refractive index. The refraction effects will thus be different for the different Bloch waves, i. This has been studied in detail for the solid/vacuum interface (Kato & Uyeda, 1951; Lehmpfuhl & Reissland, 1968), and used to determine the mean inner potential as well as structure factors using small crystals of regular shape. An expression for the potential energy has been derived by Gjønnes, Hafnor & Høier (1971):

$$U^i = U_0 - 2K\gamma^i + \sum_g |C_g^i|^2 2Ks_g.$$

Here γ^i is the *Anpassung*, C_g^i the Bloch-wave

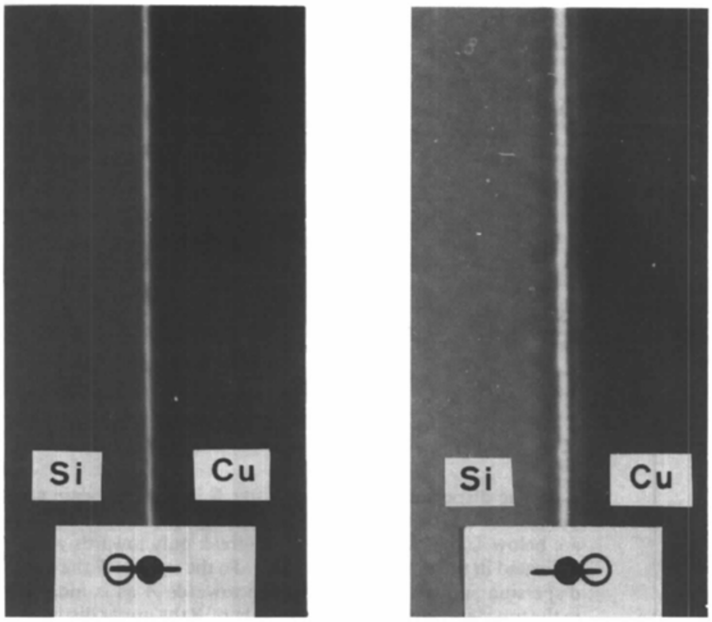

(a) (b)

Fig. 2. Dark-field images of the Si(100)/SiO_2/Cr/Cu sandwich. The position of the objective aperture is indicated with an open circle. (a) The Si/SiO_2 interface. (b) The SiO_2/Cr and the faint Cr/Cu interface separated by 40 Å.

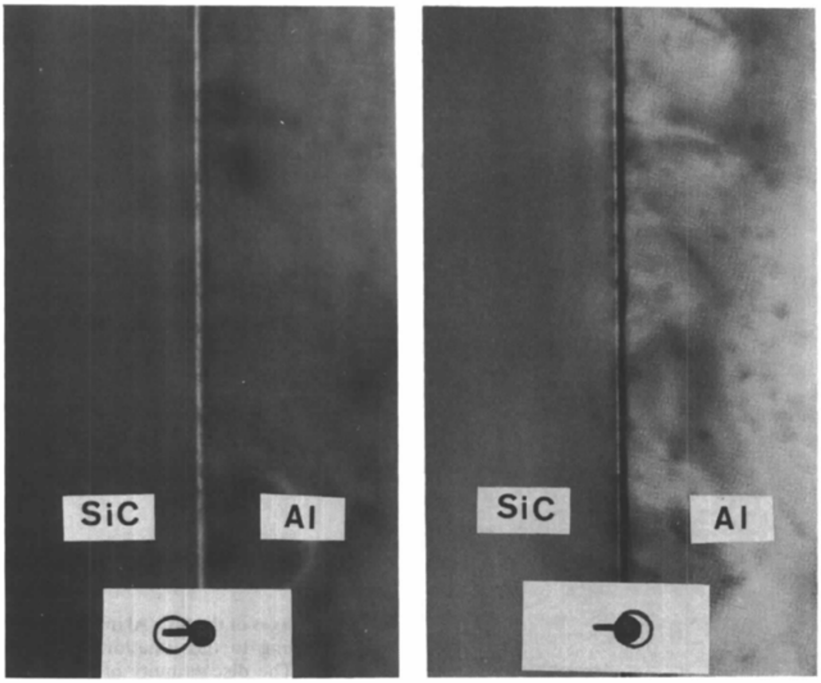

(a) (b)

Fig. 3. The SiC/Al interface for an Al matrix containing SiC particles. (a) Dark-field image. (b) Bright-field image.

coefficients, s_g the excitation error and K the wave vector of the incident electrons. Fig. 4 shows a two-beam example when the reflection is at the Bragg position. This example suggests that the two Bloch waves will be deflected in opposite directions. The condition for total reflection may be derived from Fig. 5. Owing to the presence of a Bragg reflection in crystal B the wave vectors of the two Bloch waves are $K_{z,B}+\gamma^{1,2}$. With the net planes normal to the

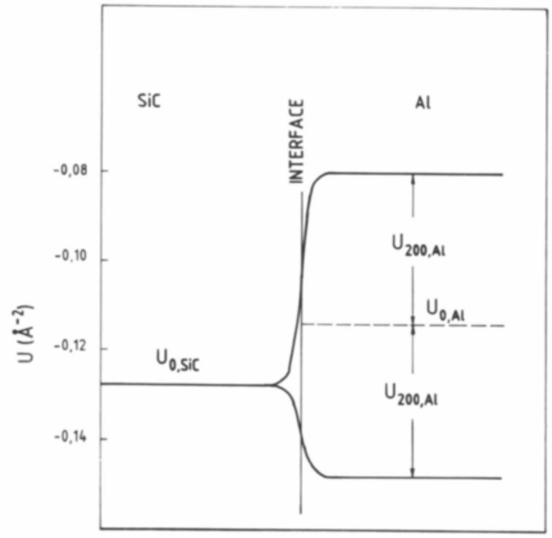

Fig. 4. The potentials of the fast electrons at the SiC/Al interface when the 200 reflection of Al is at the Bragg position.

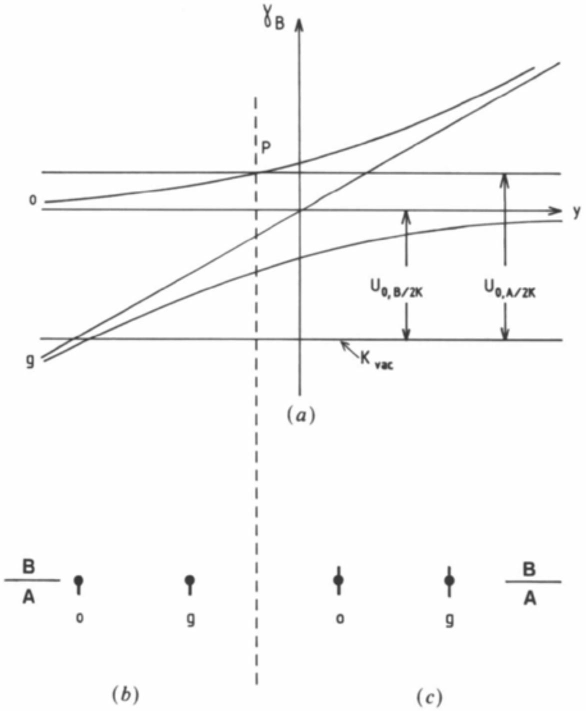

Fig. 5. The dispersion surface of crystal B in the two-beam case. To the left of the vertical dotted line through P both surfaces are below $U_{0,A}/2K$ giving rise to a streak only towards A as is indicated in the top view (lower left). To the right of P the upper dispersion surface gives a deflection towards A as is indicated in the top view (lower left). To the right of P the upper dispersion surface gives a deflection towards B (lower right).

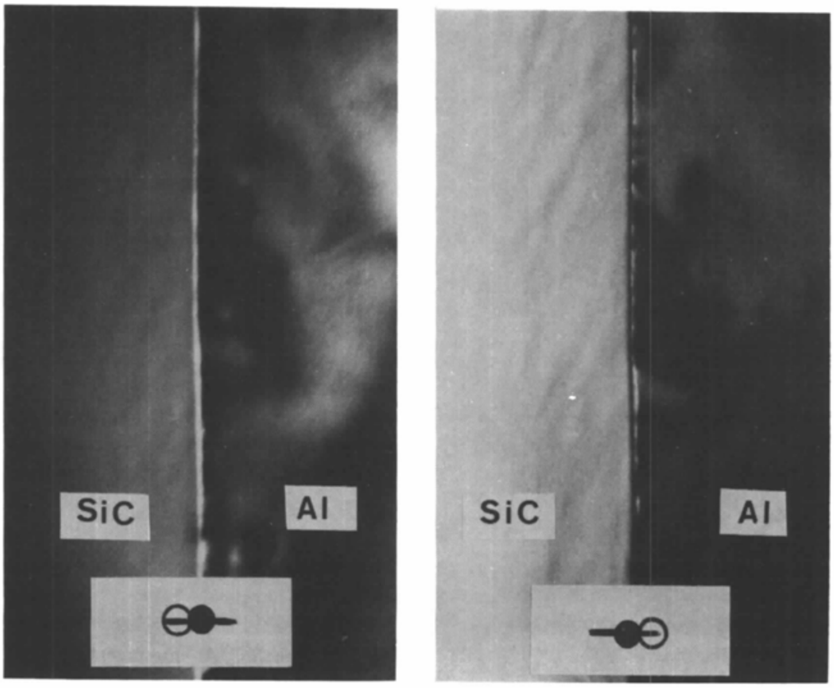

(a) (b)

Fig. 6. Images of the SiC/Al interface corresponding to the situation shown in Fig. 4. The discontinuity of the bright line in (b) is caused by strain in the Al crystal.

interface (for simplicity in the drawing) $\gamma^{1,2}$ will vary with the incident wave-vector component K_y parallel to the surface as sketched. In a simple two-beam case, the total reflection of the wave in A will prevail to the left of point P, the condition for which is given by

$$U_{0,B} - U_{0,A} = Ks_g + [(Ks_g)^2 + U_g^2]^{1/2},$$

where s_g is negative. To the right of this point the wave in A can penetrate into B, whereas the upper Bloch wave in B will be reflected off the interface. Bloch waves become weakly excited when $|\gamma| > U_g/2K$ and thus the deflection towards B is clearly visible in the diffraction pattern only when $\Delta U_0 < U_g$. Fig. 6 shows this effect experimentally for the SiC/Al interface. The 200 reflection of Al is strongly excited, but bending and distortions of the Al crystal result in a local variation of the excitation error of Al along the interface. Thus, whereas a continuous bright line is observed when the objective aperture is displaced towards the SiC crystal (Fig. 6*a*), the bright line is discontinuous when the objective aperture is displaced towards Al (Fig. 6*b*), as one should expect when the excitation error varies sufficiently.

Quantitative determination of the mean inner potential difference at an interface requires a more ideal interface where the diffraction conditions can be determined accurately from the Kikuchi lines or the band contours. Also, many-beam dynamical calculations are necessary for at least one of the phases at the interface, or, in most cases, for both phases if both are crystalline.

Discussion

Reflection and refraction of fast electrons is presented as a novel technique to study buried interfaces. The technique is sensitive to a thin layer of a third phase at the interface between two phases, as is evident from the ease with which a 12 Å layer of SiO_2 is detected between Si and Cr (Fig. 2*a*). Observation of the interface between Cr and Cu (Fig. 2*b*) suggests that the technique is also sensitive to very small differences in mean inner potential ΔU_0. In particular, the technique offers the possibility of determining the mean inner potential U_0 of crystalline as well as amorphous phases through ΔU_0 appearing at interfaces. U_0 is not easy to calculate because it depends strongly on the distribution of outer electrons and is therefore very sensitive to the electronic structure of the solid. Previous experimental methods rely mainly upon refraction through crystals with perfect external shape, MgO being the standard example (Lehmpfuhl & Reissland, 1968).

The method presented here is simple, notably in the determination of ΔU_0. With present techniques for preparing thin films and cross sections it appears possible to establish a series of inner potentials against which other substances may be tested.

Accurate measurement of the magnitude of ΔU_0 relies on the Bragg diffraction effects in one of the phases at the interface. The excitation error at which one Bloch wave starts to be deflected in the opposite direction (point P in Fig. 5) must then be measured in the Kikuchi pattern or the bend contours. This is feasible when $2\Delta U_0/|(U_{0,A} + U_{0,B})| < 0{\cdot}25$, as may be evident from Fig. 4. Thus this technique cannot be used on an external surface.

In a previous paper Taftø, Jones & Heald (1986) pointed out the possibility of performing electron energy-loss spectroscopy in the low-energy-loss region (plasmon spectrum). For that purpose a large ΔU_0 is favorable in order to enhance the intensity of the deflected electrons, and thus the intensity of the interface energy-loss signal.

The theoretical treatment given here is quite simple and essentially qualitative. It is based upon comparing wave fields set up on either side of an interface nearly parallel to the incident beam. When tangential continuity of the wave vectors across the interface can be obtained, it is assumed that the wave fields can be joined up and propagation across the interface can take place. This should be seen as an approximation to the mathematical boundary problem associated with the solution of the wave equation in the interfacial region. However, quantitative expressions for the diffracted wave from the interfacial region may be obtained by introducing the wave field inherent in the present formulation into the integral equation for scattering.

References

BATSON, P. E., KAVANGH, K. L., WODALL, J. M. & MAYER, J. W. (1986). *Phys. Rev. Lett.* **57**, 2729-2732.

COWLEY, J. M. & MOODIE, A. F. (1957). *Acta Cryst.* **10**, 609-619.

COWLEY, J. M. & TURNER, P. S. (1981). *Ultramicroscopy*, **6**, 125-138.

GJØNNES, J., HAFNOR, O. A. & HØIER, R. (1971). *Jernkontorets Ann.* **155**, 471-472.

KATO, N. & UYEDA, R. (1951). *Acta Cryst.* **4**, 227-229.

KRAKOW, W., WETZEL, J. T. & SMITH, D. A. (1986). *Philos. Mag. A*, **53**, 739-754.

LEHMPFUHL, G. & REISSLAND, A. (1968). *Z. Naturforsch. Teil A*, **23**, 544-549.

OURMAZD, A., TAYLOR, D. W., RENTSCHLER, J. A. & BEVK, J. (1987). *Phys. Rev. Lett.* **59**, 213-216.

TAFTØ, J., JONES, R. H. & HEALD, S. M. (1986). *J. Appl. Phys.* **60**, 4316-4318.